The impact of lactose type on disintegration: An integral study on porosity and polymorphism

Janssen, Pauline; Berardi, Alberto; Kok, Jurien H.; Thornton, Anthony W. ; Dickhoff, Bastiaan

Published in:
European Journal of Pharmaceutics and Biopharmaceutics

DOI:
10.1016/j.ejpb.2022.10.012

Publication date:
2022

European Journal of Pharmaceutics and Biopharmaceutics 180 (2022) 251–259

Contents lists available at ScienceDirect

European Journal of Pharmaceutics and Biopharmaceutics

journal homepage: www.elsevier.com/locate/ejpb

Research paper

The impact of lactose type on disintegration: An integral study on porosity and polymorphism

Pauline H.M. Janssen [a,b,*], Alberto Berardi [a], Jurjen H. Kok [a], Anthony W. Thornton [c], Bastiaan H.J. Dickhoff [a]

[a] DFE Pharma, Klever Strasse 187, 47568 Goch, Germany
[b] Department of Pharmaceutical Technology and Biopharmacy, University of Groningen, Antonius Deusinglaan 1, 9713 AV Groningen, The Netherlands
[c] Micromeritics Instrument Corporation, 4356 Communications Drive, Norcross, GA 30093-2901, United States

ARTICLE INFO

Keywords:
Excipients
Formulation
Pharmaceutics
Lactose
Disintegration
Pore size distribution
Dissolution
Tablet porosity

ABSTRACT

Besides factors such as disintegrant and lubricant, the raw material properties of filler excipients can have an impact on the disintegration behavior of a tablet. The current research aims to model the impact of lactose properties on disintegration time. For the first time, the impact of lactose polymorphism, tablet tensile strength, and pore structure parameters on disintegration were evaluated in one study. Six different lactose qualities were compacted into tablets of different solid fractions in a formulation with 5 %w/w diclofenac sodium, 1 %w/w magnesium stearate and 2 %w/w croscarmellose sodium. A linear model was built to identify which parameters impact the disintegration time, using as potential variables the polymorphic composition of the lactose, the porosity, pore size distribution and the tablet tensile strength. The model variables were derived from literature and calibrated with data. After optimization, the model shows a strong correlation (r^2 = 0.982) between measured and predicted disintegration times. Among all investigated variables, the polymorphic composition of lactose, and the pore size distribution have been identified to affect tablet disintegration most. A higher concentration of lactose monohydrate in tablets leads to faster tablet disintegration, explained by the slower dissolution rate of lactose monohydrate compared to anhydrous and amorphous lactose. Tablet tensile strength was not identified as a direct driver for disintegration. Instead, the pore size distribution is a mutual driver for both tablet tensile strength and disintegration. The obtained insights provide guidance on the importance of quality attributes of filler binders for the prediction of tablet disintegration. This study can therefore be used as a starting point for quality-by-design formulation development and for the development of mechanistic models to predict tablet disintegration.

1. Introduction

A key challenge in the development of oral dosage forms is to assure adequate dissolution of the active pharmaceutical ingredient (API). Especially for drugs belonging to BCS Class II and IV, poor dissolution can limit the bioavailability of the drug, thereby affecting the therapeutic efficacy [1]. Dissolution of tablets is usually preceded by disintegration, which makes disintegration critical for performance. Tablet disintegration is the process of breaking up a compact into smaller particles [2]. This results in an increase in surface area available for dissolution and subsequently absorption. For a rapidly dissolving immediate release formulation with a highly soluble drug, the drug release rate is even proposed to be fully controlled by the disintegration rate of the tablet [3].

Typically, disintegrants are added to a formulation to aid the disintegration. Disintegrants are commonly classified in literature as traditional disintegrants and superdisintegrants [4]. The term superdisintegrants refers to disintegrants that have improved efficacy and facilitate faster disintegration with smaller quantity, compared to regular disintegrants. The most widely used superdisintegrants are synthetic polymers such as crospovidone (XPVP), modified starches such as sodium starch glycolate (SSG), and modified cellulose derivatives such as croscarmellose sodium (CCS) [5–7]. The main mechanisms of action for (super-) disintegrants are wicking, swelling and shape recovery [6–9]. Wicking is the phenomenon of water penetration enhancement by drawing water into a tablet due to the presence of

* Corresponding author.
E-mail addresses: pauline.janssen@dfepharma.com (P.H.M. Janssen), tony.thornton@micromeritics.com (A.W. Thornton).

https://doi.org/10.1016/j.ejpb.2022.10.012
Received 4 July 2022; Received in revised form 28 September 2022; Accepted 12 October 2022
Available online 18 October 2022

hydrophilic groups [10]. Wicking itself does not result in a pressure that can rupture particle–particle bonds, but it is a prerequisite to initiate other mechanisms like swelling or shape recovery [9]. Swelling is the three-dimensional enlargement of particles by hydration. Shape recovery relates to the reversible process of deformation of compacted particles. Mechanical activation in this case leads to (partial) recovery of the original shape of a particle that was deformed upon compression [11]. The pressure generated by swelling or shape recovery pushes apart adjoining components and the tablet matrix breaks when the cohesive or adhesive forces between particles of the ingredients are overcome [6].

CCS is an effective superdisintegrant with a predominant wicking mechanism, followed by swelling. The low cohesiveness and compressibility of the material provides tablet porosity with pathways for the penetration of fluid [4]. CCS is typically more effective in soluble matrices, due to the fast distribution of water throughout the tablet matrix, leading to rapid dissolution of soluble matrix components [10].

Many researchers have evaluated the correlation between the type and proportion of disintegrants, and disintegration performance [5,6,9–11]. Besides the type and proportion of the disintegrant however, there are also many other factors in a formulation that affect the disintegration of a dosage form. These include the type and proportion of other excipients, API dose, API properties, hardness of tablet and the porosity of a tablet [11,12].

Tablet porosity has been a focus point in many investigations on tablet disintegration, due to its impact on multiple disintegration steps [13]. Tablet porosity typically has a positive effect on the wicking rate, while it can have an inhibiting effect on the tablet breakage by swelling or shape recovery [14–16]. In pharmaceutical practice the pore structure of a tablet is often described by a single parameter referring to the total pore volume or porosity [9]. The pore structure of a tablet however, cannot be accurately described by just one single parameter as one parameter cannot describe how void space is distributed over the tablet. Porous media can therefore more accurately be described by a combination of parameters or a pore size distribution. The pore size distribution can be measured by traditional porosimetry techniques using mercury intrusion [17,18]. Pore size distributions have been used successfully to explain differences in the rate of liquid uptake by MCC tablets [19]. Vromans et al. [20] showed that the pore size distribution of a tablet was affected by the compression pressure as well as the type of lactose used for compression.

It is generally accepted that filler excipients also have an impact on disintegration. For soluble fillers, the disintegration can for example be affected by the solubility, hydrophilicity, wettability and swelling of the excipient [7,21]. Lactose is an example of a filler for which differences in raw material properties can lead to differences in disintegration properties [22,23]. Van Kamp et al. [24] evaluated the dissolution and disintegration properties of different types of lactose. They found significant differences between the disintegration of pure lactose tablets. These differences were hypothesized to be the result of differences in water penetration due to the combination of small pore diameters and precipitation in the pores of alpha lactose monohydrate. Ziffels and Steckel also confirmed that the increased initial solubility of anhydrous alpha lactose can lead to increased disintegration times [25]. Vromans et al. [26] showed a similar effect for amorphous lactose, explained by the superior initial solubility of amorphous lactose compared to any crystalline lactose. The high solubility of amorphous lactose was identified to hinder water penetration into tablets by the formation of a layer of saturated lactose solution on the powder bed. In this layer crystallization to lactose monohydrate occurs, which limits the wetting of the internal part of the powder [27]. This effect was amplified for small pores, when water penetration is slow and the surface area for dissolution is large.

Although research has identified the impact of filler binder properties for tablet disintegration [11,12,21,28], recent reviews highlight the lack of understanding how variation in fillers can affect disintegration properties of actual formulations [5,7]. The current research aims to fill this gap and is unique in its integral approach. Six different lactose qualities were compacted into tablets of different solid fractions in a formulation with 5 %w/w diclofenac sodium, 1 %w/w magnesium stearate and 2 %w/w croscarmellose sodium to mimic actual formulations. A linear model was built to identify which parameters influence the disintegration time, using as potential variables the polymorphic composition of the lactose, the porosity, pore size distribution and the tablet tensile strength. Research outcomes provide guidance on the importance of quality attributes of filler binders for the prediction of tablet disintegration. It can therefore be used as a starting point for quality-by-design formulation development and for the development of mechanistic models to predict tablet disintegration.

2. Materials and methods

2.1. Materials

Spray dried lactose (SuperTab® 50ODT, SuperTab® 11SD and SuperTab® 14SD), granulated lactose (SuperTab® 30GR), anhydrous lactose (SuperTab® 21AN) and granulated anhydrous lactose (SuperTab® 24AN) were obtained from DFE Pharma (Goch, Germany). Formulations were prepared in portions of 500 g by blending 92 % w/w lactose with 5 % w/w diclofenac sodium (Fagron, Rotterdam) and 2 % w/w croscarmellose sodium (DFE Pharma, Goch, Germany) in a Turbula blender (Turbula T2F, Willy A. Bachofen, Basel, Switzerland) at 90 rpm for 8 min. Lubrication was performed by adding 1 % w/w magnesium stearate (Sigma Aldrich, Missouri) and blending for another 2 min at 90 rpm in a Turbula blender.

2.2. Lactose characterization

The apparent amorphous content (n = 2) of the lactose grades was measured by differential scanning calorimetry (Mettler Toledo, Columbus, USA). Approximately 5 mg of lactose was weighted in a sealed cup with 5 mg acid casein and heated from 25 °C till 95 °C with 5 °C/min. The heat of crystallization was used to calculate the amorphous content. The beta content of lactose (n = 2) was determined by gas chromatography (Agilent, Santa Clara, USA) according to method 2.2.28 in the Ph. Eur. lactose monograph. Particle size distributions were determined (n = 3) by dry laser diffraction (Helos/KR, Sympatec, Germany) using a dispersion unit with a feed rate of 50 % and an air pressure of 0.5 bar. The specific surface area was determined (n = 2) by Krypton BET on a TriStar II Plus (Micromeritics, Norcross, USA). Analyses were performed with an equilibrium interval of 10 s over a normalized pressure range of 0.05–0.3.

2.3. Tableting

Tablets were compressed on a Rotab T rotary tablet press (Luxner, Berlin, Germany) with five punches rotating at 25 rpm with an optifiller speed of 13 rpm. Tableting was performed at 5 kN, 10 kN, 15 kN and 20 kN to target solid fractions of 0.75, 0.80, 0.85 and 0.90. Tablets are compressed using flat beveled 9 mm punches (iHolland, Nottingham, UK). The filling depth of the die was set such that tablets of a weight of 250 mg +/− 2 mg were obtained. Samples were taken after running at equilibrium for 2 min.

2.4. Tablet analyses

2.4.1. Tablet crushing strength

Tablets (n = 20) were analyzed on tablet crushing strength (TCS), weight, diameter and thickness by using an automated tablet tester (Sotax AT50, Aesch, Switzerland). Force to break the tablet was measured at constant speed of 120 mm/min (2 mm/s), max force needed to break the tablets was used as crushing force. 20 tablets are analyzed and average and standard deviation is reported. The tablet tensile

strength (TTS) was calculated because this value is independent of tablet size. Tablet tensile strength (TTS) can be derived from the tablet crushing strength (TCS), diameter (D) and tablet thickness (t) for flat beveled tablets [29]:

$$TTS = \frac{2 \bullet TCS}{\pi \bullet D \bullet t} \quad (1)$$

2.4.2. Tablet solid fraction

The skeletal density (n = 3) of 10 cm^3 bulk powder blends was tested with an AccuPyc pycnometer (Micromeritics, Norcross, USA). Each sample was purged (n = 10) with Helium to prepare, and the skeletal volume was determined (n = 10) with equilibration determined by rate of pressure change. The solid fraction (SF) was calculated from the skeletal density (ρ_{true}) and the tablet mass (mass) and volume (V) according to:

$$SF = \frac{mass}{V} / \rho_{true} \quad (2)$$

in which the tablet volume (V) of flat beveled tablets is calculated from the tablet radius (r) and tablet thickness (t):

$$V = \pi \bullet r^2 \bullet t \quad (3)$$

The porosity (φ) of tablets is calculated according to:

$$\varphi = 1 - SF \quad (4)$$

2.4.3. Tablet disintegration

Tablet disintegration time was measured on a disintegration tester ZT122 (Erweka, Langen, Germany). Six tablets were tested and time was reported in seconds when tablet is dissolved.

2.4.4. Mercury intrusion porosimetry

Three tablets were characterized (n = 2) by a full intrusion analysis on an AutoPore V (Micromeritics, Norcross, USA), with a maximum pressure of 400 MPa, followed by extrusion back to atmospheric pressure. Equilibration was determined by rate of intrusion. The p10, p50 and p90 were defined as the pore size diameters at which 10 %, 50 % and 90 % of the total intrusion volume is intruded.

2.5. Modelling disintegration time

Model development was performed to identify which parameters that are impacted by the filler-binder choice have the most impact on disintegration time. The model was developed with twelve datapoints, originating from six different formulations that are tableted towards two different porosities of 15 % and 20 %. A second model is created with the same six formulations tableted towards porosities of 10 % and 25 %. The reason for creating two binary linear models, rather than having a single non-linear model is that four different levels of porosity were not sufficient to develop a robust non-linear model. The two simplified linear models are expected to provide only semi-quantitative information on which are the critical factors controlling the disintegration time of tablet exclusively within the confined space of the tested formulations.

The amorphous content (L_{am}), anhydrous beta content (L_{beta}), porosity (φ), the pore size diameters at which 10 %, 50 % and 90 % of the total intrusion volume was intruded (p_{10}, p_{50}, p_{90}), the tablet tensile strength (TTS), the median particle size (x_{50}), the specific surface area (SSA) and a constant (Z) were used as potential parameters for the linear model to predict the disintegration time (DT_{pred}):

$$DT_{pred} = \boldsymbol{a} \bullet L_{am} + \boldsymbol{b} \bullet L_{beta} + \boldsymbol{c} \bullet \varphi + \boldsymbol{d} \bullet p_{10} + \boldsymbol{e} \bullet p_{50} + \boldsymbol{f} \bullet p_{90} + \boldsymbol{g} \bullet TTS + \boldsymbol{h} \bullet x_{50} + \boldsymbol{i} \bullet SSA + \boldsymbol{Z} \quad (5)$$

The Generalized Reduced Gradient (GRG) non-linear solver method was used to optimize parameters *a-Z* and minimize the difference between the predicted disintegration time (DT_{pred}) and the measured disintegration time (DT_m):

$$\sum_{i=1}^{12} (DT_m - DT_{pred})^2 \quad (6)$$

Boundary conditions were derived from mechanistic knowledge. Amorphous content and anhydrous lactose both have a positive correlation with disintegration time, as they increase the disintegration time by having increased solubility [24–26]. Tablet tensile strength as a measure for bonding strength has a positive correlation with disintegration time [20].

$$\boldsymbol{a} \geq 0, \boldsymbol{b} \geq 0 \; and \; \boldsymbol{g} \geq 0 \quad (7)$$

The strength of the model was evaluated by calculating the mean absolute percentage error (MAPE) from the predicted disintegration times (DT_{pred}) and the measured disintegration times (DT_m) over *n* observations by:

$$MAPE = \frac{1}{n} \sum_{n} \frac{|DT_m - DT_{pred}|}{|DT_m|} * 100\% \quad (8)$$

The MAPE was used to optimize the model and to reduce the amount of parameters contributing to the prediction by the following steps. Firstly, parameters that contributed < 10 % of the maximally contributing parameters were set to 0. The contribution of a factor was determined by the difference between the maximum and minimum value of a parameter times the defined slope for this parameter. Thereafter, it was verified one by one which parameters can be removed while keeping the MAPE below 10 %. When multiple parameters could be removed while complying to this criterion, it was evaluated which of these parameters can jointly be removed to keep the MAPE below 10 %, and as low as possible.

2.6. Evaluation of the impact of lactose polymorphism

2.6.1. Wicking behavior

Tablets were qualitatively evaluated on wicking behavior with a camera. Two petri dishes were filled up to a height of 2.5 mm with liquid containing a few drops of Cresyl violet acetate (Sigma Aldrich, Saint Louis, Missouri, USA). One petri dish contained water with Cresyl violet acetate, one contained saturated lactose solution with Cresyl violet acetate. For each analysis, tablets were carefully put into the solution and every 30 s an image was captured with a microscope camera (DNT, Leer, Germany).

2.6.2. Tableting conditioned spray dried lactose

Spray dried lactose grades 11SD and 14SD were placed in a climate chamber at 40 °C/75 %RH for 24 h to convert the amorphous lactose into crystalline lactose monohydrate. Absence of amorphous content was confirmed by DSC testing (as described in section 2.2). Lumps in the products were broken by passing through a 300 μm sieve. These materials were processed into blends and tableted and tested as described before (sections 2.1, 2.3, and 2.4).

3. Results

3.1. Lactose polymorphism

The anomeric composition and amorphous content of lactose grades is summarized in Table 1. Spray dried lactose grades contained amorphous lactose in concentrations between 8 and 14 % w/w. The beta content of anhydrous lactose and granulated anhydrous lactose were around 80 % w/w, while for the other lactose grades this was below 15 % w/w.

3.2. Tablet characterization

The compressibility, compactibility and tabletability of the six formulations containing different lactose qualities are summarized in Fig. 1. Compressibility differences for the different lactose formulations were below 2 % at all compression pressures. Spray dried lactose (50ODT, 11SD and 14SD) had the highest compressibility, followed by granulated lactose monohydrate (30GR) and anhydrous lactose (21AN, 24AN) respectively.

Compactibility and tabletability were both the highest for 24AN, followed by 14SD and 21AN respectively. Disintegration properties of the produced tablets are shown in Fig. 2. At a given solid fraction (or compaction pressure), fastest disintegration was observed for 30GR, followed by 50ODT and 11SD respectively. 24AN had the highest disintegration time.

Tablet pore size distributions of the analyzed tablets are provided in Supplementary Fig. 1. The p10, p50 and p90 of the pore size distributions are summarized in Table 3. Tablets with similar solid fractions showed a different pore size distribution. For both solid fractions, the pore size distribution of 50ODT, 11SD and 30GR started at a larger pore diameter than for 14SD, 21AN and 24AN. Tablets with solid fraction 0.80 generally had a higher p10 than tablets with solid fraction 0.85, indicating a larger proportion of large pores. 14SD and 24AN with solid fraction 0.80 were the exception on this, as the p10 for these tablets was in the same range as the p10 for 50ODT, 11SD and 30GR with solid fraction 0.85. At both solid fractions, 24AN had the largest proportion of fine pores, followed by 14SD.

3.3. Modelling disintegration time

An overview of the parameters that were used for modelling are provided in Supplementary Table 1. The resulting coefficients from each modelling step are summarized in Supplementary Table 2. Coefficients **c, d** and **i** for porosity, p10 and specific surface area respectively, were set to 0 after the first iteration, due to their contribution which was below 10 % of the maximum contributing parameter. In the second step, parameter **f** was also removed, due to the contribution being below 10 % of the maximum contributing parameter. In the third step, parameters were removed one by one to evaluate the impact on the model. Removal of parameters **a** or **b** for amorphous content and anhydrous content resulted in a significant drop in explanatory power with an MAPE value above 15 %. Removal of parameter **e, g** or **h** resulted in a minimal increase in MAPE to 4.2–8.0 %. When parameters **e**, **g**, and **h** jointly were removed, the MAPE increased to a value of 19 %. When two out of three parameters were removed, the MAPE remained below 10 % for two combinations, with the lowest MAPE for inclusion of parameter **e**. Final model was therefore constructed with the most relevant parameter from these, being parameter **e**. The final model that was selected therefore predicts the disintegration time (DT_{pred}) of this system based upon the amorphous content (L_{am}), anhydrous content (L_{beta}), and the pore size diameter at which 50 % of the total intrusion volume is intruded (p_{50}) according to:

$$DT_{pred} = 14.7 \bullet L_{am} + 2.9 \bullet L_{beta} - 314 \bullet p_{50} + 214 \quad (9)$$

Fig. 3 shows the correlation between the measured disintegration times and the predicted disintegration times with the optimized model. A strong correlation between the two was observed, in line with the low MAPE of 4.8 % for this model.

A second modelling exercise was performed with additional data from 10 % and 25 % porosity tablets to confirm the significance of the previous findings. The performed steps of this modelling approach are provided in Supplementary Table 3. The resulting model from this evaluation predicts the disintegration time (DT_{pred}) of this system based upon the amorphous content (L_{am}), anhydrous content (L_{beta}), and the pore size diameter at which respectively 50 % and 90 % of the total intrusion volume was intruded (p_{50}, p_{90}) according to:

$$DT_{pred} = 13.2 \bullet L_{am} + 1.5 \bullet L_{beta} + 220 \bullet p_{50} - 1993 \bullet p_{90} + 318 \quad (10)$$

The validity of the model approach is confirmed by best subset and regression analysis in Minitab which resulted in the same regression equation (data not shown).

3.4. Wicking in a saturated lactose solution

The wicking behavior of 24AN and 30GR tablets was visualized to create additional understanding on the impact of lactose solubility on disintegration mechanism. Fig. 4 shows the wicking of 24AN and 30GR tablets in water and in a saturated lactose solution. In both cases, wicking of 30GR was faster than for 24AN, while erosion at the surface of the tablets was more severe for 24AN than for 30GR. Wicking towards the core and erosion at the surface of the tablets were both reduced when a saturated lactose solution is used. The erosion of 24AN tablets was faster than that of 30GR tablets.

3.4.1. Conditioning of spray dried lactose

Spray dried lactose grades 11SD and 14SD were placed in a climate chamber at 40 °C/75 %RH for 24 h to remove the amorphous content, as confirmed by DSC measurements. Fig. 5 shows the tabletability and the tablet disintegration as function of the tensile strength for both conditioned and unconditioned formulations. Higher tablet tensile strength was obtained for non-conditioned material, when amorphous lactose is present. Faster disintegration however, was obtained by the use of conditioned spray dried lactose grades.

Fig. 6 shows the wicking behavior of 11SD and conditioned 11SD

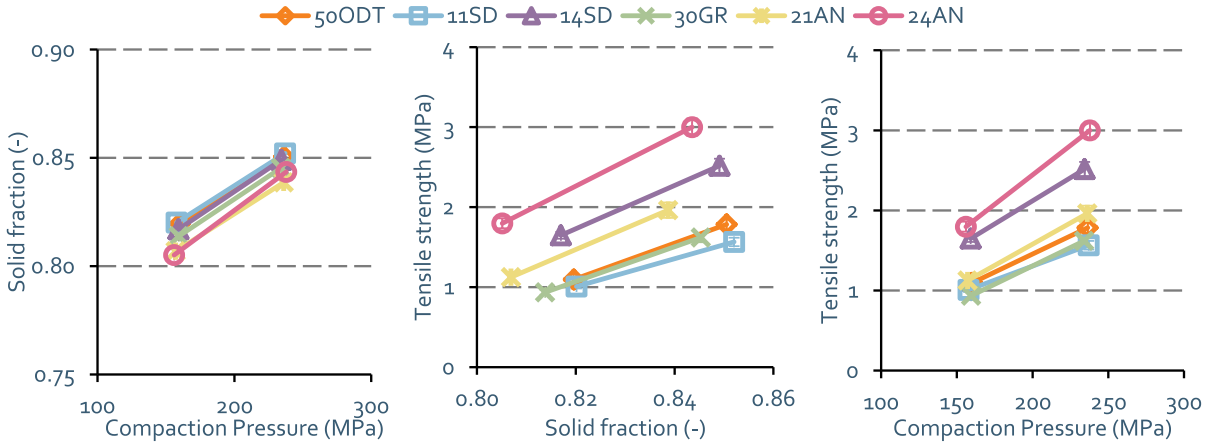

Fig. 1. Tableting properties of six formulations with different lactose grades, showing the compressibility (left), compactibility (middle) and tabletability (right).

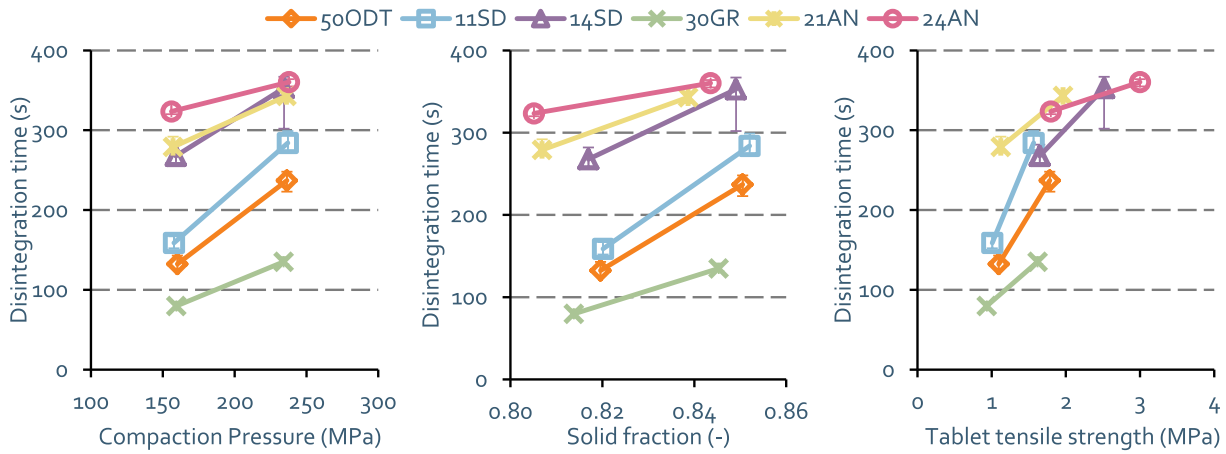

Fig. 2. Tablet disintegration of the six different formulations, as function of compaction pressure (left), solid fraction (middle), and tablet tensile strength (right). Error bars on disintegration indicate the first and last of 6 tablets.

Table 1
Formulation compositions indicating the type of lactose that is used. Tablets from formulation X with a target solid fraction of 0.80 and 0.85 are indicated X1 and X2 respectively.

Formulation	Lactose grade	Lactose type	Other ingredients in all formulations
50ODT	SuperTab® 50ODT	Spray dried	5 % w/w diclofenac sodium +
11SD	SuperTab® 11SD	Spray dried	2 % w/w croscarmellose sodium +
14SD	SuperTab® 14SD	Spray dried	1 % w/w magnesium stearate
30GR	SuperTab® 30GR	Granulated	
21AN	SuperTab® 21AN	Anhydrous	
24AN	SuperTab® 24AN	Granulated anhydrous	

(11SD*) in water and in a saturated lactose solution. In both cases, wicking of conditioned 11SD was significantly faster than for unconditioned 11SD. Wicking towards the core of the tablets was reduced when a saturated lactose solution was used.

4. Discussion

4.1. Tablet characterization

Spray dried lactose had a slightly higher ability to reduce volume upon compression compared to anhydrous or granulated lactose, which is explained by the structure of spray dried lactose. Spray dried lactose consists of crystals of fine α-lactose monohydrate in a plastically deforming amorphous matrix [20,30]. This partial plastic deformation contributes to a reduction in volume upon compression. Due to the small differences in compressibility, compactibility is the main driver for differences in tabletability. All six evaluated formulations are suitable for direct compression, indicated by the tablet tensile strength greater than 1.5 MPa at a solid fraction of 0.85. Generally, a tablet tensile

Table 3
Pore size distribution parameters p10, p50 and p90 for the different tablets.

Formulation	Tablets with solid fraction 0.80			Tablets with solid fraction 0.85		
	p10 (μm)	**p50 (μm)**	**p90 (μm)**	**p10 (μm)**	**p50 (μm)**	**p90 (μm)**
50ODT	1.26	0.66	0.15	0.82	0.39	0.10
11SD	1.50	0.74	0.16	0.99	0.41	0.11
14SD	0.99	0.55	0.13	0.64	0.28	0.09
30GR	1.21	0.57	0.15	0.94	0.34	0.10
21AN	1.02	0.55	0.15	0.79	0.33	0.10
24AN	0.91	0.43	0.12	0.52	0.24	0.08

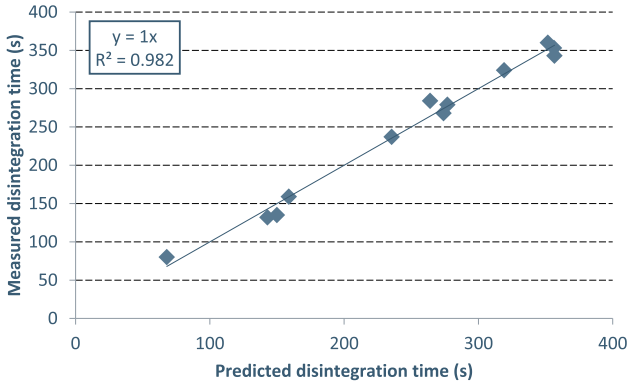

Fig. 3. Correlation graph between the predicted disintegration time and the measured disintegration time.

Table 2
Anomeric composition, median particle size and specific surface area of the different lactose grades used in this study. Spray dried grades contain amorphous regions of lactose, while anhydrous lactose mainly contains beta lactose.

Formulation	Lactose grade	Lactose type	Amorphous (w/w%)	Beta content (w/w%)	Median particle size (μm)	Specific surface area (m^2/g)
50ODT	SuperTab® 50ODT	Spray dried	8.3	6.4	120	0.21
11SD	SuperTab® 11SD	Spray dried	10.1	8.4	112	0.21
14SD	SuperTab® 14SD	Spray dried	13.4	12.3	124	0.30
30GR	SuperTab® 30GR	Granulated	0	13.2	114	0.29
21AN	SuperTab® 21AN	Anhydrous	0	83.4	132	0.38
24AN	SuperTab® 24AN	Granulated anhydrous	0	77	93	0.46

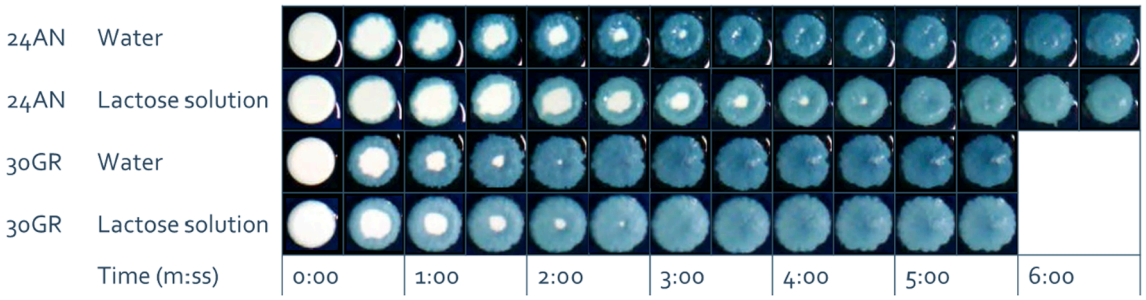

Fig. 4. Wicking behavior of 24AN tablets and 30GR tablets withs solid fraction 0.80 in water and a saturated lactose solution. Wicking of 30GR is faster than for 24AN, and for both tablets wicking is faster in water than in a saturated lactose solution.

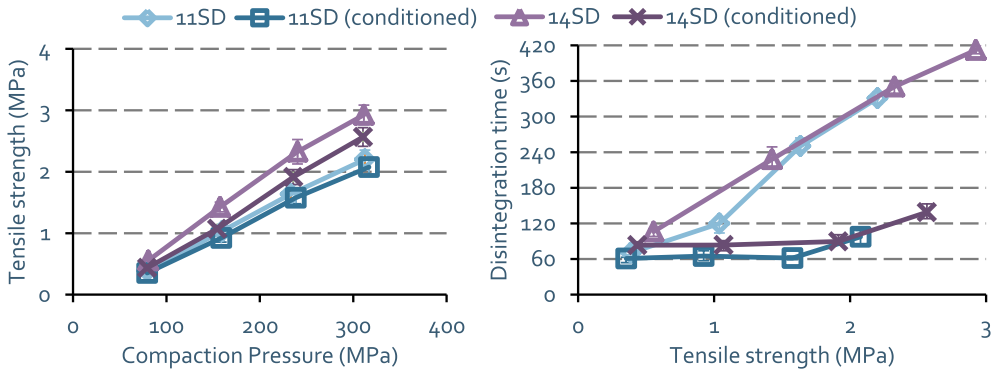

Fig. 5. Tablet disintegration of two different spray dried formulations, with and without conditioning the raw material to remove the amorphous content before processing. Error bars on disintegration indicate the first and last of 6 tablets.

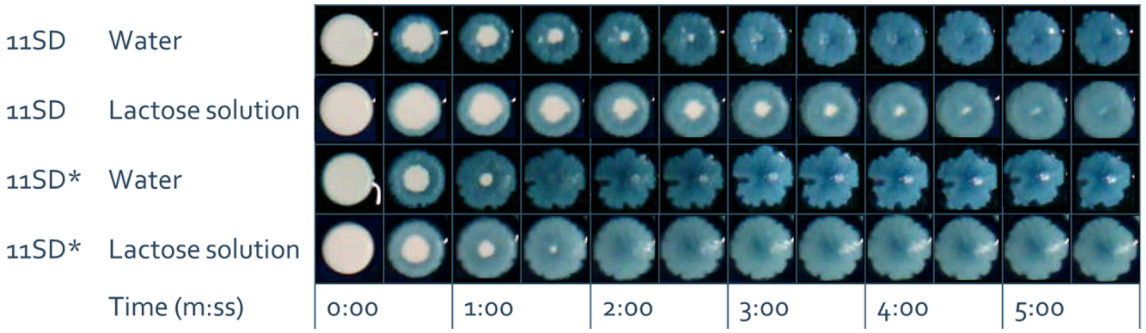

Fig. 6. Wicking behavior of 11SD tablets and conditioned 11SD (11SD*) tablets with solid fraction 0.80 in water and a saturated lactose solution. Wicking is faster for conditioned 11SD, and for both tablets wicking is faster in water than in a saturated lactose solution.

strength greater than 1.0 MPa will indicate that the tablet is mechanically strong enough to withstand commercial manufacturing process stresses and subsequent stresses during distribution [29].

Compactibility and tabletability were both the highest for 24AN, followed by 14SD and 21AN respectively. The increased compactibility and subsequently tabletability for 21AN and 24AN is explained by the morphology of anhydrous lactose. Anhydrous lactose is produced by roller drying and has a rough surface structure with clusters of microcrystals in shard-shaped particles. Anhydrous lactose demonstrates better compaction behavior than α-lactose monohydrate, due to the presence of rougher surfaces and a higher degree of fragmentation [27,31]. 24AN showed the highest compactibility, due to the additional granulation step that is performed during production of the used lactose grade. Agglomeration by granulation is known to improve the compactibility of brittle materials, because of the increased fragmentation propensity [32]. This effect is further strengthened by a 20 % higher specific surface area, indicating additional surface available for bonding upon compaction. A similar difference in compaction behavior was observed when comparing the 50ODT, 11SD and 14SD; which contain spray dried lactose. Spray dried lactose consists of crystals of fine α-lactose monohydrate with an imperfect crystal structure in a plastically deforming amorphous matrix [31]. The compaction properties of spray dried lactose increases when the primary particle size is smaller, due to the larger surface present for bonding and the change from brittle to ductile compaction behavior when particle size is reduced [33,34]. Indeed, the spray dried grade 11SD is produced with a primary particle size of 20 μm, whereas the spray dried lactose grade of 14SD is produced with a primary particle size of approximately 34 μm [34]. This decrease in primary particle size results in a 40 % higher specific surface area and 60 % higher tabletability.

4.2. Modelling disintegration time

All tablets disintegrated within six minutes, which is in line with

typical disintegration times of immediate-release tablets [9]. At a given solid fraction, fastest disintegration was observed for 30GR, followed by 50ODT and 11SD respectively. Modelling the disintegration time resulted in significant positive contribution for amorphous lactose and anhydrous lactose. Amorphous lactose has a higher contribution than anhydrous lactose, which was expected due to the higher solubility [24–26].

Two mechanisms are described to explain how the higher solubility of amorphous or beta lactose can have a negative impact on disintegration. These two mechanisms, being the increased blockage of pores by re-crystallization and the increased competition for water, are described in more detail below. The contribution of both these mechanisms is unknown and it is proposed to evaluate this in a follow-up study.

The first mechanism of increased blockage of pores by re-crystallization is visualized in Fig. 7 and can be understood by evaluating the solubility of alpha and beta lactose separately. The initial solubility of alpha lactose in 100 mL water at 20 °C is 7 g, while the initial solubility of beta lactose at the same conditions is 50 g [35]. When beta lactose dissolves, part of the dissolved beta lactose mutarotates to alpha lactose until the equilibrium ratio of 62.7 % beta and 37.3 % alpha is obtained. When 50 g of beta lactose is dissolved, this results in 30.8 g of beta lactose and 19.2 g of alpha lactose in the solution. In this case the solution is supersaturated with alpha lactose, while being below the saturation point of beta lactose. Therefore, alpha lactose will crystallize from the solution until only 7 g of dissolved alpha lactose is left in the solution, while beta lactose is continues to dissolve. At the same time, mutarotation towards alpha lactose followed by crystallization also continues. The process of dissolution of beta lactose, followed by mutarotation and crystallization continues until all beta is dissolved and the equilibrium alpha/beta ratio in solution is obtained. On a microscopic scale in the tablet, the intermediate recrystallization of alpha lactose leads to narrowing of pores, which decelerates the water penetration into the tablet.

The second mechanism that can explain why higher solubility of amorphous or beta lactose can limit the disintegration is described as increased competition for water and is visualized in Fig. 8. This mechanism focuses on the amount of freely available water molecules and hydration kinetics of excipients [28]. The competition for water theory describes that soluble fillers bind a large number of water molecules in hydrate shells and prevent, therefore, proper disintegrant action [28]. This would mean that if the solubility of an ingredient is higher in the liquid, more molecules are available to bind water molecules in hydrate shells and disintegration times are increased [36].

The modelling approach also showed that pore size distribution has a significant effect on tablet disintegration. Porosity, p50 and p90 all showed a significant contribution on the disintegration time. As these parameters are correlated however, one parameter appeared to be sufficient to include in the model. Median pore size gave the best correlation, with p10 as the second best parameter. Including the porosity instead of p50 in the model increased the MAPE from 5.3 % to 14.6 %, showing that the distribution of pore volume over the tablet is more relevant for disintegration than just the porosity. The importance of pore diameter is in line with the Lucas-Washburn equation, that describes the penetration of water into a porous system, assuming that pores are uniform and cylindrical [37]. In this case, the penetration length (y) as function of time (t) can be expressed for a laminar flow as function of the contact angle between the water and the solid component (θ), the dynamic viscosity of water (η), the surface tension of water (γ) and the hydraulic radius (Rh,eq), which is defined as the ratio between the pore volume to the solid–fluid interfacial area:

$$y(t) = \sqrt{\frac{R_{h,eq} \bullet \gamma \bullet \cos\theta t}{2 \bullet \eta}} \quad (11)$$

Water penetration therefore depends more on the pore size diameter than on the porosity. An inverse relationship between the median pore size diameter and disintegration time was observed. This is explained by a strong contribution from increased wicking at high median pore size compared to the reduced pressure build-up after swelling at high median pore size. This effect is even more pronounced when anhydrous and amorphous lactose is present, as a smaller median pore size also increases the risk for pore blockage.

Interestingly, literature on surface energy suggest that the contact angle for alpha lactose monohydrate would be higher than the contact angle for beta anhydrous lactose [38]. According to equation 11, a higher contact angle results in slower water penetration, which is in contrast to the observed differences in disintegration time. This shows that surface energy has a relatively low impact on the disintegration

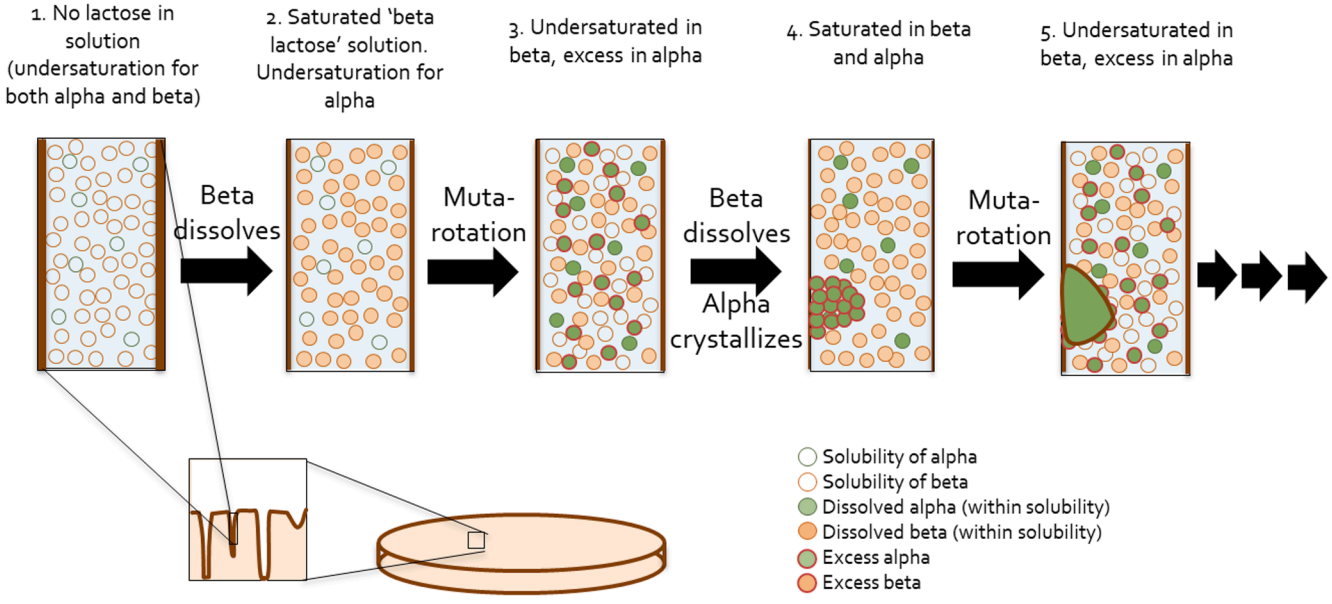

Fig. 7. The increased risk for narrowing of pores by re-crystallization after dissolution of beta lactose. On a microscopic scale, there is a continuous process of dissolution of beta lactose, followed by mutarotation to alpha lactose and recrystallization. The recrystallization towards alpha crystals could lead to narrowing of pores, which could hinder the water penetration through the tablet.

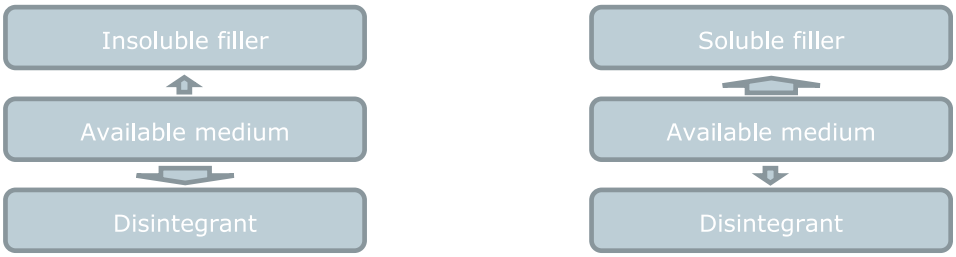

Fig. 8. Illustration of the competition-for-water hypothesis for a mixture of disintegrant with an insoluble, hydrophilic filler and a mixture of disintegrant with a soluble, hydrophilic filler.

time in this formulation, compared to the impact from solubility differences via the competition of water or the recrystallization theory.

A second modelling exercise was performed with additional data from 10 % and 25 % porosity tablets to confirm the previous findings. Analyses of these tablets are not combined with analyses from 15 % and 20 % porosity, to exclude disturbances from non-linear effects. The second model contains the same parameters as the first model, except an additional parameter for p90. The first model indicated a negative correlation with the median pore size p50 of −313. The second model indicated a positive correlation with median pore size of + 220, with an additional negative correlation with the p90 of −1993. As the p50 of these tablets is 2.7 to 4.7 times larger than the p90, the total correlation of the pore size distribution is negative in both models. Furthermore, both models show a larger impact for amorphous lactose than for anhydrous lactose, which is related to the higher initial solubility of this polymorph. Overall, the second model confirmed the findings of the first model, as similar parameters were identified as relevant.

A finding of this modelling approach was the absence of a causal relation between tablet tensile strength and tablet disintegration. A high bonding strength between particles was expected to limit tablet disintegration, but apparently these differences do not contribute on top of the already identified variables. Typically, a small median pore size indicates tight bonding and a high tensile strength, while large pores correlate to a lower tensile strength. Tablet tensile strength was therefore not identified as a direct driver for disintegration, but as a parameter with a mutual driver of median pore size diameter.

An important remark is that the current models are developed based upon one model formulation, produced by direct compression. Further research is recommended to evaluate if the same parameters have a significant contribution when used in other formulations and with other processing technologies. Especially the disintegrant type and disintegrant concentration are expected to play a crucial role.

4.3. Wicking in a saturated lactose solution

Visualization of the wicking into tablets clearly showed differences in erosion and wicking when a lactose grade with different solubility was used. The predominantly present anhydrous beta lactose in 24AN has a higher initial solubility than alpha lactose monohydrate in 30GR, which leads to more visible erosion of 24AN tablets. Additionally, the slower wicking for 24AN confirms that the solubility of a filler can have a negative effect on disintegration, either via the increased recrystallization or via the increased competition for water.

For both tablet compositions, saturation of the disintegration liquid with lactose results in a decrease of wicking speed. Saturation of the disintegration liquid leads to faster oversaturation of lactose in the tablet pores, which is hypothesized to lead to more recrystallization of the lactose. The saturation of the disintegration liquid also reduces the amount of freely available water molecules, which could reduce the wicking speed via the competition for water theory. Further research to distinguish between these two mechanisms is recommended.

4.4. Conditioning of spray dried lactose

Storage at 40 °C and 75 % RH for 24 h of spray dried lactose grades 11SD and 14SD resulted in complete removal of the amorphous content, in line with known crystallization behavior of amorphous lactose [39]. The removal of the plastically deforming amorphous matrix was shown to reduce the tabletability of spray dried lactose grades 11SD and 14SD. In parallel, the removal resulted in faster disintegration for the tablets. For tablets with a tensile strength of 2 MPa, a three-fold reduction in tablet disintegration time was obtained. Additionally, significantly faster wicking and less erosion was observed for tablets produced from conditioned 11SD compared to tablets produced from non-conditioned 11SD. These findings are line with the findings in Section 4.2 that also showed slower disintegration times with amorphous lactose present.

5. Conclusions

For the first time, the impact of lactose polymorphism, tablet hardness and pore structure parameters were evaluated in one study. A linear model with a strong correlation (r^2 = 0.982) between measured and predicted disintegration times was developed. Among all factors that were investigated, the polymorphic composition of lactose, and the pore size distribution have been identified to affect tablet disintegration the most. The presence of amorphous lactose and anhydrous lactose in lactose monohydrate tablets can increase the disintegration time, due to the higher solubility of these polymorphs. Additionally, the pore size distribution has been identified to have an effect on tablet disintegration. A finding of this modelling approach was the absence of a direct correlation between tablet tensile strength and tablet disintegration. Tablet tensile strength was not identified as a direct driver for disintegration, but merely as a parameter with a mutual driver of pore size distribution. The obtained insights provide guidance on the importance of quality attributes of filler binders for the prediction of tablet disintegration. It can therefore be used as a starting point for quality-by-design formulation development and for the development of mechanistic models to predict tablet disintegration.

Declaration of Competing Interest

The authors declare that they have no known competing financial interests or personal relationships that could have appeared to influence the work reported in this paper.

Data availability

Data will be made available on request.

Acknowledgements

We thank Jack Saad, Amalia Thomas, Laura Shaw, Katharina Peikert and Laura Monington for assistance with characterization of the raw materials. We also thank prof. dr. H.W. Frijlink for his diligent proofreading of the article.

References

[1] D. Bhowmik, R. Bhanot, K.P.S. Kumar, Recent trends in role of superdisintegrants to formulation of solid oral dosage form, Res. J. Pharm. Dos. Forms Technol. 10 (2018) 245, https://doi.org/10.5958/0975-4377.2018.00036.8.

[2] D.A. Silva, G.K. Webster, N. Bou-Chacra, R. Löbenberg, The significance of disintegration testing in pharmaceutical development, Dissolution Technol. 25 (3) (2018) 30–38.

[3] B. Nickerson, A. Kong, P. Gerst, S. Kao, Correlation of dissolution and disintegration results for an immediate-release tablet, J. Pharm. Biomed. Anal. 150 (2018) 333–340, https://doi.org/10.1016/j.jpba.2017.12.017.

[4] C. Moreton, Disintegrants in tableting, in: L.L. Augsburgern, S.W. Hoag (Eds.), Pharm. Dos. Forms, CRC Press, 2008: pp. 233–266.

[5] J. Quodbach, P. Kleinebudde, A critical review on tablet disintegration, Pharm. Dev. Technol. 21 (2016) 763–774, https://doi.org/10.3109/10837450.2015.1045618.

[6] P.M. Desai, C.V. Liew, P.W.S. Heng, Review of Disintegrants and the Disintegration Phenomena, J. Pharm. Sci. 105 (2016) 2545–2555, https://doi.org/10.1016/j.xphs.2015.12.019.

[7] A. Berardi, L. Bisharat, J. Quodbach, S. Abdel Rahim, D.R. Perinelli, M. Cespi, Advancing the understanding of the tablet disintegration phenomenon – An update on recent studies, Int. J. Pharm. 598 (2021) 120390.

[8] C. Caramella, P. Colombo, U. Conte, F. Ferrari, A. La Manna, H.V. Van Kamp, G. K. Bolhuis, Water Uptake and Disintegratng Force Measurements: Towards a General Understanding of Disitnegration Mechanisms, Drug Dev. Ind. Pharm. 12 (1986) 1749–1766.

[9] D. Markl, J.A. Zeitler, A Review of Disintegration Mechanisms and Measurement Techniques, Pharm. Res. 34 (2017) 890–917, https://doi.org/10.1007/s11095-017-2129-z.

[10] P.S. Mohanachandran, P.G. Sindhumol, T.S. Kiran, Superdisintegrants: An overview, Int. J. Pharm. Sci. Rev. Res. 6 (2011) 105–109.

[11] H. Shihora, S. Panda, Superdisintegrants, Utility in Dosage Forms : A Quick Review, J. Pharm. Sci. Biosci. Res. 1 (2011) 148–153.

[12] R. Shegokar, C. Wiebinga, Eye on Excipients: Journey of widely used superdisintegrant - sodium starch glycolate, Tablets Capsul. (2015).

[13] Y.X. Bi, H. Sunada, Y. Yonezawa, K. Danjo, Evaluation of rapidly disintegrating tablets prepared by a direct compression method, Drug Dev. Ind. Pharm. 25 (1999) 571–581, https://doi.org/10.1081/DDC-100102211.

[14] H. Nogami, J. Hasegawa, M. Miyamoto, Studies on Powdered Preparations. XX. Disintegration of the Aspirin Tablets containing Starches as Disintegrating Agent, Chem. Pharm. Bull. 15 (3) (1967) 279–289.

[15] H. Sunada, Y. Bi, Preparation, evaluation and optimization of rapidly disintegrating tablets, Powder Technol. 122 (2002) 188–198, https://doi.org/10.1016/S0032-5910(01)00415-6.

[16] W. Lowenthal, Pharmaceutical sciences Disintegration of Tablets, 61 (1972) 1695–1711.

[17] P.A.C. Gane, C.J. Ridgway, E. Lehtinen, R. Valiullin, I. Furó, J. Schoelkopf, H. Paulapuro, J. Daicic, Comparison of NMR cryoporometry, mercury intrusion porosimetry, and DSC thermoporosimetry in characterizing pore size distributions of compressed finely ground calcium carbonate structures, Ind. Eng. Chem. Res. 43 (2004) 7920–7927, https://doi.org/10.1021/ie049448p.

[18] A.B. Selkirk, D. Ganderton, An investigation of the pore structure of tablets of sucrose and lactose by mercury porosimetry, J. Pharm. Pharmacol. 22 (1970) 79S–85S, https://doi.org/10.1111/j.2042-7158.1970.tb08584.x.

[19] M. Al-Sharabi, D. Markl, T. Mudley, P. Bawuah, A.-P. Karttunen, C. Ridgway, P. Gane, J. Ketolainen, K.-E. Peiponen, T. Rades, J.A. Zeitler, Simultaneous investigation of the liquid transport and swelling performance during tablet disintegration, Int. J. Pharm. 584 (2020) 119380.

[20] H. Vromans, A.H. De Boer, G.K. Bolhuis, C.F. Lerk, K.D. Kussendrager, H. Bosch, Studies on tableting properties of lactose - Part 2. Consolidation and compaction of different types of crystalline lactose, Pharm. Weekbl. Sci. Ed. 7 (1985) 186–193, https://doi.org/10.1007/BF02307575.

[21] N. Maclean, E. Walsh, M. Soundaranathan, I. Khadra, J. Mann, H. Williams, D. Markl, Exploring the performance-controlling tablet disintegration mechanisms for direct compression formulations, Int. J. Pharm. 599 (2021) 120221.

[22] DFE Pharma, Primojel - In direct compression, (n.d.). https://dfepharma.com/Excipients/Expertise/Oral-Solid-Dose/Superdisintegrants/Primojel (accessed November 24, 2021).

[23] DFE Pharma, Primellose - In direct compression, (n.d.). https://dfepharma.com/Excipients/Expertise/Oral-Solid-Dose/Superdisintegrants/Primellose (accessed November 24, 2021).

[24] H.V. van Kamp, G.K. Bolhuis, K.D. Kussendrager, C.F. Lerk, Studies on tableting properties of lactose. IV. Dissolution and disintegration properties of different types of crystalline lactose, Int. J. Pharm. 28 (2-3) (1986) 229–238.

[25] S. Ziffels, H. Steckel, Influence of amorphous content on compaction behaviour of anhydrous _ -lactose, Int. J. Pharm. 387 (2010) 71–78, https://doi.org/10.1016/j.ijpharm.2009.12.009.

[26] H. Vromans, G.K. Bolhuis, C.F. Lerk, K.D. Kussendrager, Studies on tableting properties of lactose. VIII. The effect of variations in primary particle size, percentage of amorphous lactose and addition of a disintegrant on the disintegration of spray-dried lactose tablets, Int. J. Pharm. 39 (1987) 201–206, https://doi.org/10.1016/0378-5173(87)90217-1.

[27] H. Vromans, G.K. Bolhuis, C.F. Lerk, H. van de Biggelaar, H. Bosch, Studies on tableting properties of lactose. VII. The effect of variations in primary particle size and percentage of amorphous lactose in spray dried lactose products, Int. J. Pharm. 35 (1987) 29–37, https://doi.org/10.1016/0378-5173(87)90071-8.

[28] N. Ekmekciyan, T. Tuglu, F. El-Saleh, C. Muehlenfeld, E. Stoyanov, J. Quodbach, Competing for water: A new approach to understand disintegrant performance, Int. J. Pharm. 548 (2018) 491–499, https://doi.org/10.1016/j.ijpharm.2018.07.025.

[29] K.G. Pitt, M.G. Heasley, Determination of the tensile strength of elongated tablets, Powder Technol. 238 (2013) 169–175, https://doi.org/10.1016/j.powtec.2011.12.060.

[30] C.F. Lerk, Consolidation and compaction of lactose, Drug Dev. Ind. Pharm. 19 (17-18) (1993) 2359–2398.

[31] J.F. Gamble, W.S. Chiu, V. Gray, H. Toale, M. Tobyn, Y. Wu, Investigation into the degree of variability in the solid-state properties of common pharmaceutical excipients-anhydrous lactose, AAPS PharmSciTech. 11 (2010) 1552–1557, https://doi.org/10.1208/s12249-010-9527-4.

[32] K. Zuurman, K.A. Riepma, G.K. Bolhuis, H. Vromans, C.F. Lerk, The relationship between bulk density and compactibility of lactose granulations, Int. J. Pharm. 102 (1994) 1–9, https://doi.org/10.1016/0378-5173(94)90033-7.

[33] G.K. Bolhuis, N.A. Armstrong, Excipients for direct compaction - An update, Pharm. Dev. Technol. 11 (2006) 111–124, https://doi.org/10.1080/10837450500464255.

[34] G. Bolhuis, K. Kussendrager, J. Langridge, New developments in spray-dried lactose, Pharm. Technol. EXCIPIENTS SOLID Dos. FORMS 2004 (2004) 26.

[35] P.F. Fox, T. Uniacke-Lowe, P.L.H. McSweeney, J.A. O'Mahony (Eds.), Dairy Chemistry and Biochemistry, Springer International Publishing, Cham, 2015.

[36] L. Bisharat, H.S. AlKhatib, S. Muhaissen, J. Quodbach, A. Blaibleh, M. Cespi, A. Berardi, The influence of ethanol on superdisintegrants and on tablets disintegration, Eur. J. Pharm. Sci. 129 (2019) 140–147, https://doi.org/10.1016/j.ejps.2019.01.004.

[37] D. Markl, P. Wang, C. Ridgway, A.P. Karttunen, P. Bawuah, J. Ketolainen, P. Gane, K.E. Peiponen, J.A. Zeitler, Resolving the rapid water absorption of porous functionalised calcium carbonate powder compacts by terahertz pulsed imaging, Chem. Eng. Res. Des. 132 (2018) 1082–1090, https://doi.org/10.1016/j.cherd.2017.12.048.

[38] D. Traini, P.M. Young, F. Thielmann, M. Acharya, The influence of lactose pseudopolymorphic form on salbutamol sulfate-lactose interactions in DPI formulations, Drug Dev. Ind. Pharm. 34 (2008) 992–1001, https://doi.org/10.1080/03639040802154889.

[39] R. Price, P.M. Young, Visualization of the Crystallization of Lactose from the Amorphous State, J. Pharm. Sci. 93 (2004) 155–164, https://doi.org/10.1002/jps.10513.